Effect of H_2S inhibition on the hydrodechlorination of polychlorinated biphenyls over Mo/Al_2O_3 and $Co–Mo/Al_2O_3$ catalysts

Marjorie De La Rosa, Paulino Betancourt, Armando Díaz, Joaquín L. Brito & Susana Pinto-Castilla

Reaction Kinetics, Mechanisms and Catalysis

ISSN 1878-5190

Reac Kinet Mech Cat
DOI 10.1007/s11144-013-0635-5

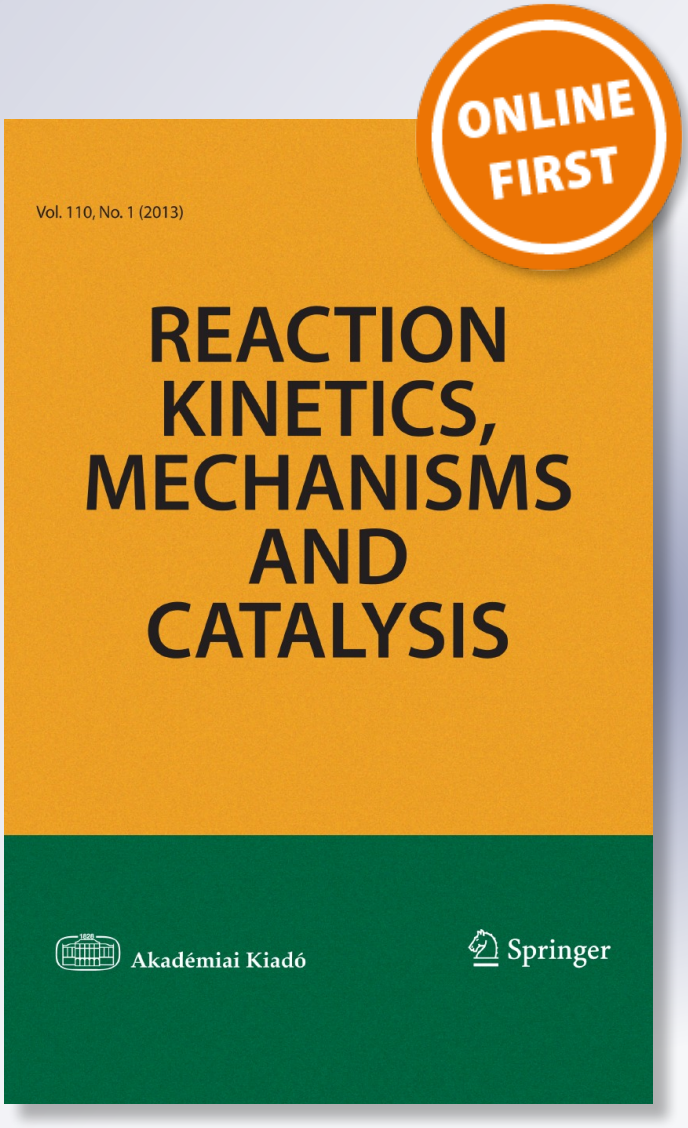

Springer

Reac Kinet Mech Cat
DOI 10.1007/s11144-013-0635-5

Effect of H_2S inhibition on the hydrodechlorination of polychlorinated biphenyls over Mo/Al_2O_3 and $Co–Mo/Al_2O_3$ catalysts

Marjorie De La Rosa · Paulino Betancourt · Armando Díaz · Joaquín L. Brito · Susana Pinto-Castilla

Received: 16 April 2013 / Accepted: 28 September 2013

Abstract The effect of the cobalt addition on the H_2S inhibition and subsequently on the polychlorinated biphenyl (PCB) hydrodechlorination (HDC) activity over Mo-based catalysts was investigated. The HDC activity over a Mo catalyst containing cobalt was much higher than that over the same Mo catalyst without cobalt. On the other hand, the HDC activity of the Co–Mo catalyst was more inhibited by H_2S than that of the Mo catalyst at 300 °C. Thus, kinetic parameters were calculated using a Langmuir–Hinshelwood model to determine the reaction pathway of the H_2S inhibition over Mo and Co–Mo catalysts. We found that the heats of adsorption of PCB (Aroclor® 1242) and H_2S on the Co–Mo catalyst was higher than on the Mo catalyst, indicating that the sulfur-containing species adsorb more strongly on the catalyst containing cobalt. The results suggested that while the Co–Mo catalyst was more inhibited by H_2S, the Mo–S bonds were more stable on this catalyst than on the solely Mo catalyst. This Mo–S bond was responsible for the stabilization of the active phase, which allowed creation of a greater amount of sulfur atoms potentially labile. Thus, that explained the better HDC activity over the Co–Mo catalyst than over the Mo catalyst, despite a greater H_2S inhibition on the former.

M. De La Rosa · P. Betancourt (✉) · S. Pinto-Castilla
Centro de Catálisis, Petróleo y Petroquímica, Escuela de Química, Facultad de Ciencias, Universidad Central de Venezuela, Los Chaguaramos, AP 40679, Caracas, Venezuela
e-mail: paulino.betancourt@ciens.ucv.ve

A. Díaz
Gerencia de Ecología y Ambiente, PDVSA-Intevep, El Tambor, Estado Miranda, Venezuela

J. L. Brito · S. Pinto-Castilla
Centro de Química, Instituto Venezolano de Investigaciones Científicas (IVIC), Altos de Pipe, Caracas 1020-A, Estado Miranda, Venezuela

Published online: 17 October 2013

Keywords Aroclor 1242 · Co–Mo catalyst · H_2S inhibition · Hydrodechlorination · Langmuir–Hinshelwood model · Polychlorinated biphenyls

Introduction

Polychlorinated biphenyls (PCBs) were commercially produced since 1929 through the mid 1970s. They are a group of nonpolar chlorinated hydrocarbons with a biphenyl moiety on which 1–10 of the hydrogen atoms have been replaced by chlorine. Commercial PCBs were manufactured and sold as complex mixtures containing multiple isomers at different degrees of chlorination, for such uses as transformer oil, hydraulic and heat transfer fluid, and as components of paints. PCBs are widespread and persistent, they bioaccumulate and pose a risk of causing adverse effects to human health and to the global ecosystem [1–5]. While a substantial amount of the world production (ca. 1.5 million tons) has been destroyed, the major part still remains in use or awaits destruction, whilst a substantial proportion has been released to the environment. Because of the high thermodynamic, chemical and biological stability of PCBs, all degradation methods are extremely difficult [3]. Furthermore, as is clear from the report commissioned by the Environment Programme of the United Nations, many countries still do not have suitable PCB disposal or treatment facilities [6]. Therefore, an effective remediation methodology for PCBs is a critical factor for future protection from improper disposal or accidental leaks (e.g. fire, earthquake) of stored PCBs. Currently, they are mainly being destroyed by high-temperature incineration, but public concerns about discharges from incinerators are strongly forcing a move to chemical methods [3, 7–9]. Chemical remediation techniques currently under development include substitution of chlorides [10] hydride reduction, [11–13], dechlorination [14–17], dechlorination using metals [18–22], photolysis [23], γ-radiolysis [24–28], oxidation [29], electrolysis [30, 31] and supercritical degradation [32, 33]. Some of them are used commercially to treat mainly liquid PCBs, and PCB containing-oils.

Catalytic hydrodechlorination (HDC) has been studied for treating liquid wastes contaminated by chlorine-containing organic compounds such as: chlorinated olefins, chlorinated benzenes, chlorophenols, polychlorinated biphenyls (PCBs), polychlorinated dibenzo-para-dioxins (PCDDs) and polychlorinated dibenzofurans (PCDFs) [34–39]. A summary of the studies examining hydrodechlorination of both chlorinated aromatics and chlorinated alkanes and olefins has been reported [40, 41]. Due to the low operating temperatures and to the reuse of the products the HDC process is economically advantageous compared to incineration [42]. Experimental tests carried out on full scale plants have confirmed the effectiveness of the process [43]. Noble and other transition metal catalysts on silica and alumina supports have been generally employed to promote HDC reactions [40].

Presulfided hydrotreating catalysts, of the same formulation as those used in the oil refining industry for hydrodesulfurization (HDS) processes, have generally been adopted in HDC studies of chlorinated aromatics giving high hydrodechlorination levels at relatively mild operating conditions ($250 < T < 350$ °C and

$50 < P_{H2} < 100$ bar) in comparison to incineration [38–40, 44]. The main advantages of hydrotreating catalysts are low price, stability, ready availability and long duration. The results of these studies have showed that the HDC process is effective in attaining the hydrodechlorination of PCBs giving as main reaction product biphenyl.

Kinetic studies on the HDC of chlorinated benzenes show that if a low concentration of reactants is adopted and hydrogen pressure is kept constant, the assumption of first order kinetics is adequate [35, 36]. The same assumption holds true when PCBs are treated [38, 39, 45]. However, in the case of highly chlorinated PCBs the HDC reaction network can be very complex. In fact, the formation of the final product (i.e. biphenyl) takes place through many reaction steps each of them seemingly involving the substitution of a single chlorine atom.

It is well known that H_2S, which is a product of the HDS reaction, inhibits the hydrodesulfurization reaction of organic sulfur compounds such as dibenzothiophene and 4,6-dimethyldibenzothiophene [46–51]. However, to the best of our knowledge, the inhibiting effect of H_2S on the HDC of PCBs using catalysts has not been studied. In that sense, the aim of this paper is to investigate on the inhibiting effect of H_2S on HDC of PCBs (Aroclor® 1242) over a Mo-based catalyst and Co–Mo catalyst, supported on alumina. A Langmuir–Hinshelwood model for the reactions rates was applied in order to examine the kinetics of the H_2S inhibition.

Experimental

All the reagents and solvents were used as purchased without further purification.

The molybdenum-supported catalyst (9 wt% Mo) was prepared by the incipient wetness impregnation method. An appropriate amount of ammonium heptamolybdate (AHM) (Fluka AR grade) was dissolved in NH_4OH solution for impregnation of γ-Al_2O_3, followed by drying in air at 150 °C and calcination at 500 °C (surface area: 255 $m^2\ g^{-1}$).

The other examined catalyst in the present study was the oxidic commercially available Co–Mo/γ-Al_2O_3 catalyst (TK-554; Co, 2.3 wt%; Mo, 9.4 wt%) from Haldor-Topsoe A/S, with BET surface area of 200 $m^2\ g^{-1}$ and pore volume of 0.53 mL g^{-1}. It was crushed and sieved between 0.2 and 0.5 mm.

The experimental reaction system was designed to work under high pressure. A fixed-bed flow reactor (stainless-steel tube with an internal diameter of 16 mm) was packed with 1.0 g of catalyst particles. The catalyst was presulfided using a mixture of 2 vol% H_2S in H_2 at 300 °C for 1 h [52]. After presulfidation, the reactor was cooled down in the H_2S/H_2 stream to the desired temperature and thereafter it was pressurized with hydrogen. The reactant solution (PCBs in heptanes + CS_2) was then introduced into the reactor by means of a high-pressure liquid pump (Isco 65D). The PCB HDC reaction was carried out under the following conditions: temperature of 200–400 °C; total pressure of 3.5 MPa; WHSV of 28 h^{-1}; liquid flow rate of 32 mL h^{-1}; flow rate of H_2, 25 L h^{-1}; initial PCB concentration of 0.05–1.0 wt%; H_2S partial pressure of 0–0.3 $\times$ 10^5 Pa. The PCB concentration was controlled by changing the ratio BPC/heptane of the original liquid solution.

Aroclor® 1242 was a sample taken from laboratory stock (supplied by PDVSA-Intevep).

After steady state was reached (about 2 h), the first three samples of liquid products were collected from a gas–liquid separator every 30 min. The activity was calculated as the mean value obtained for three samples. Then, the reaction temperature was increased and after a further stabilization time of 2 h the next three samples were collected and analyzed. The same procedure was performed at each temperature.

For each set of experiments (including the effects of produced HCl and added H_2S), a back point was taken to check if any deactivation occurred. In all cases the activity value calculated for the back point was comparable to that of the original point.

The collected samples were analyzed with a GC–MS instrument (Agilent 6890/5973N) equipped with an electron capture detector (ECD) and a fused silica capillary column (HP-Ultra 2 crosslinked 5 % Ph-methyl silicone, $L = 40$ m, i.d. = 1.2 mm, film thickness = 0.33 μm). The oven temperature program was an initial hold for 1 min at 50 °C, followed by a ramp at 10 °C min^{-1}, to 300 °C and another hold for a further 3 min prior to cooling down. Calibration was performed by the method of external standards and as the final stage of sample preparation; hexadecane was added to all samples as an internal standard. The products were identified by GC–MS (HP 5973 mass detector coupled to an HP 6890 GC, equipped with an HP-5MS capillary column of 30 m × 0.25 mm, film thickness 0.25 μm).

The analysis of PCBs is rather difficult due to accuracy problems in PCB detection which are attributed to deterioration in sensitivity and background induced by interfering components in analytical media. However, we use an accepted standard method (ASTM D4059) [53].

The presence of hydrogen chloride was detected and measured both in the gas phase and on the catalyst after extraction with alkaline solutions. However, the amount of HCl measured generally did not satisfy the mass balance. On the other hand, the effect of the produced HCl over HDC was not studied in this work. In fact, it has been noted previously for Ni based catalysts particle growth and sintering as result of HDC [54–57]. This could be ascribed to a halide-induced agglomeration of Ni particles [58] due to the surface mobility of Ni–X species [59]. Therefore, a similar phenomenon could be anticipated to be occurring in the present CoMo system.

The selected model was the Langmuir–Hinshelwood kinetics that has been widely used for the hydrotreatment reactions:

$$r_{HDC} = \frac{k_{HDC} K_{PCB} P_{PCB} K_{H_2} P_{H_2}}{(1 + K_{PCB} P_{PCB} + K_{H_2S} P_{H_2S})(1 + K_{H_2} P_{H_2})} \quad (1)$$

where r_{HDC} is the rate of HDC; k_{HDC} is the rate constant of HDC; K_{PCB}, K_{H_2S}, and K_{H_2} are the adsorption equilibrium constants of PCB, hydrogen sulfide, and hydrogen, respectively; P_{PCB}, P_{H_2S} and P_{H_2} are the partial pressures of PCB, hydrogen sulfide, and hydrogen, respectively. According to the experimental conditions of the present study, Eq. 1 can be simplified. Indeed, as the hydrogen

pressure is constant, the terms relative to hydrogen can be included in the rate constant. Based on the above assumption, Eq. 1 can be changed into Eqs. 2 and 3:

$$r_{HDC} = \frac{k_{HDC} K_{PCB} P_{PCB}}{(1 + K_{PCB} P_{PCB} + K_{H_2S} P_{H_2S})} \tag{2}$$

$$\frac{1}{r_{HDC}} = \frac{K_{H_2S} P_{H_2S}}{k_{HDC} K_{PCB} P_{PCB}} + \frac{(1 + K_{PCB} P_{PCB})}{k_{HDC} K_{PCB} P_{PCB}} \tag{3}$$

In the case of the PCB HDC reactions performed without the addition of H_2S, the retarding term $K_{H_2S}P_{H_2S}$ can be neglected.

$$\frac{1}{r_{HDC}} = \frac{1}{k_{HDC} K_{PCB} P_{PCB}} + \frac{1}{k_{HDC}} \tag{4}$$

In separate experiments, we studied the spent catalysts used in the reaction of HDC by electron microscopy and chemical analysis. No apparent deactivation occurred with PCBs. Hydrochloric acid did not appear to cause catalyst deactivation. Certain quantities of coke were formed on the catalyst. An increase in the specific surface and chlorine surface concentration of the catalyst and a decrease in sulfur surface concentration were observed. During the HDC reaction, some large metal particles are formed, together with granular zones.

Results and discussion

Fig. 1 illustrates the efficiency of this catalytic system: A 1 wt% content of PCB is partially dechlorinated by the CoMo catalyst. The GC–MS chromatogram in Fig. 1b clearly shows the destruction of the higher Cl content PCB congeners of Aroclor® 1242. Note the almost complete disappearance of peaks with retention times, above 20 min in the chromatogram of panel b. However, the presence of new partially dechlorinated by-products is clear, as shown by the peaks between 5 and 15 min (2-chlorobiphenyl, 2,6-dichlorobiphenyl, trichlorobiphenyl, among others). After 2 h of reaction time, biphenyl is the major product from the hydrodechlorination of the PCB congeners, as shown by the integrated areas from the different signals. Multiple samples were analyzed with similar results.

PCB HDC activity without addition of hydrogen sulfide

In the present work, we decided to compare the H_2S inhibition over a Mo–alumina-based catalyst to the H_2S inhibition over a similar catalyst containing cobalt. First, PCB HDC reactions over the Mo/Al_2O_3 catalyst and the $Co–Mo/Al_2O_3$ catalyst were performed without addition of hydrogen sulfide for several PCBs concentrations to confirm the increasing HDC activity upon cobalt addition (compare Figs. 2, 3). The conversion of PCB over either catalyst increased with increasing temperatures and decreasing initial concentrations of PCBs. The HDC activity of the Mo/Al_2O_3 catalyst was more influenced by the initial PCBs concentration than that of the $Co–Mo/Al_2O_3$ one. Moreover, while the PCB conversion on the Mo/Al_2O_3 catalyst was just about

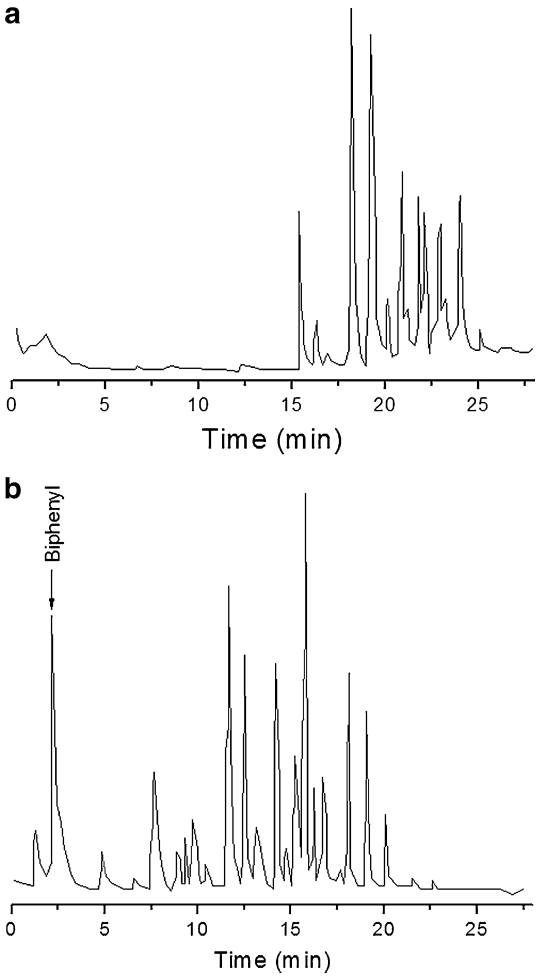

Fig. 1 Formation of biphenyl from a commercial mixture of PCB congeners, Aroclor® 1242. **a** GC/MS of Aroclor® 1242 **b** GC/MS after 2 h hydrodechlorination of Aroclor® 1242

24 % at 300 °C in the case of the experiment performed with 1 wt% PCB, the Co–Mo/Al_2O_3 catalyst exhibited an activity of about 90 % for the same experimental conditions.

In Figs. 4 and 5, we present the evolution of the fraction of PCB converted as a function of the PCB concentration in the feed for various experimental temperatures. As shown in Fig. 4, the amount of PCB converted on Mo/Al_2O_3 exhibited an increase up to 0.5 wt% PCB in the feed but leveled off when the feed was more concentrated in PCB. In contrast, the amount of PCBs converted on the Co–Mo/Al_2O_3 catalyst increased linearly with the PCB concentration in the initial feed. This means that the surface active sites present on the Mo/Al_2O_3 catalyst were saturated with PCB for a concentration of PCB of 0.5 wt% while they remained available in sufficient quantity to perform the reaction on the Co–Mo/Al_2O_3 catalyst even for a concentration of PCB of 1.0 wt%.

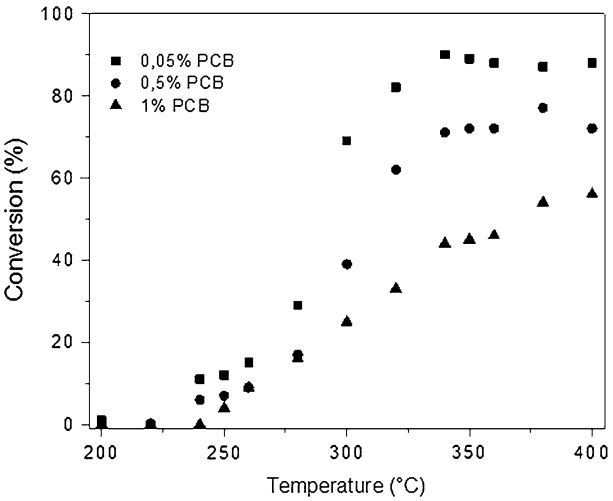

Fig. 2 Effect of the temperature on PCB conversion for various PCB concentrations. Mo/Al_2O_3 catalyst

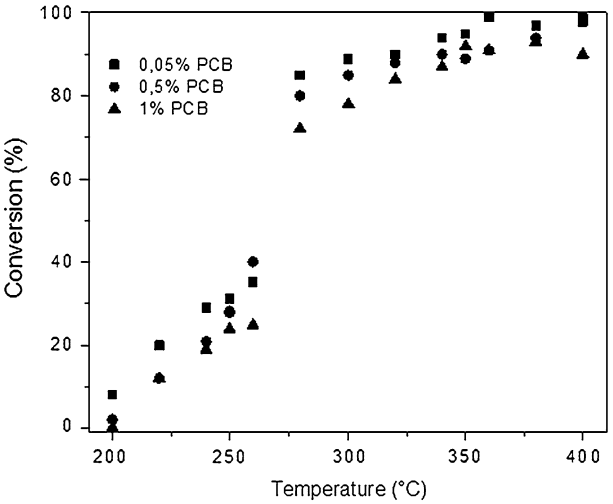

Fig. 3 Effect of the temperature on PCB conversion for various PCB concentrations. $Co–Mo/Al_2O_3$ catalyst

Results of the kinetic treatment

In order to examine whether $\frac{1}{r_{HDCl}} = \frac{1}{k_{HDCl} K_{PCB} P_{PCB}} + \frac{1}{k_{HDCl}}$ is actually adequate for the present study or not, we used it to treat our data (Eq. 4). Figs. 6 and 7 show plots representing $1/r_{HDC}$ versus $1/P_{PCB}$ for Mo/Al_2O_3 and $Co–Mo/Al_2O_3$ catalysts, respectively. The figures obtained for both catalysts exhibited linear relationships, indicating that Eq. 4 could be reliably used for the present study. Thus, k_{HDC} and

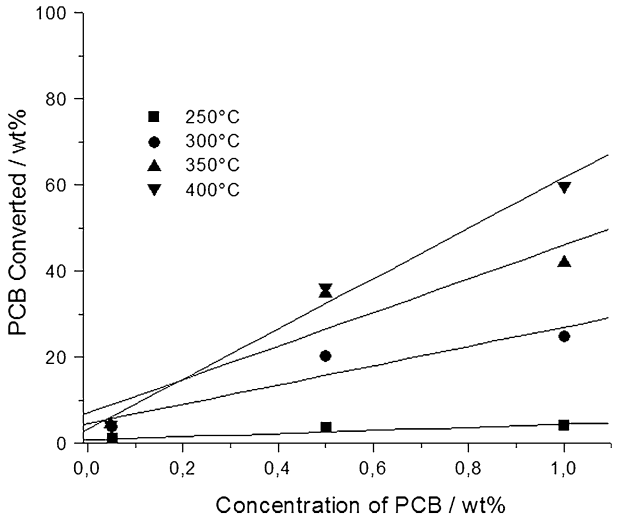

Fig. 4 Effect of the PCB concentration on the amount of PCB converted. Mo/Al_2O_3 catalyst

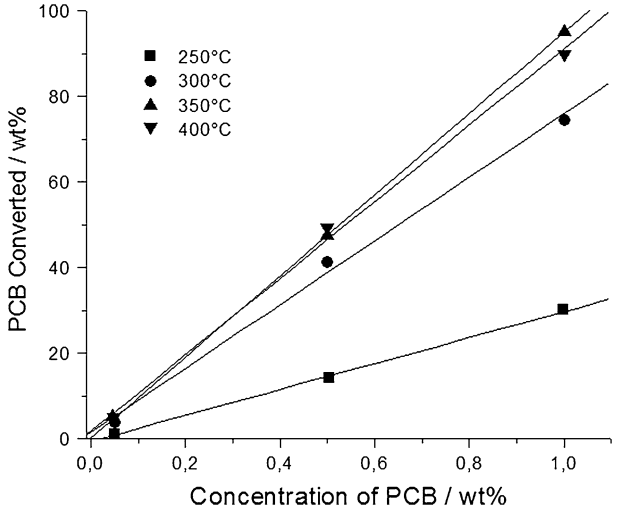

Fig. 5 Effect of the PCB concentration on the amount of PCB converted. $Co–Mo/Al_2O_3$ catalyst

K_{PCB} could be obtained upon determination of the slopes of the lines and the intercepts of the lines with the *y* axis.

Inhibiting effect of H_2S on the PCBs hydrodechlorination

The PCB HDC was carried out while adding various concentrations of H_2S that were varied in the range from 0 to 0.51 vol% (0–0.3 $\times$ 10^5 Pa). Equation 4 was used to treat the results. The obtained lines for a PCB initial concentration of

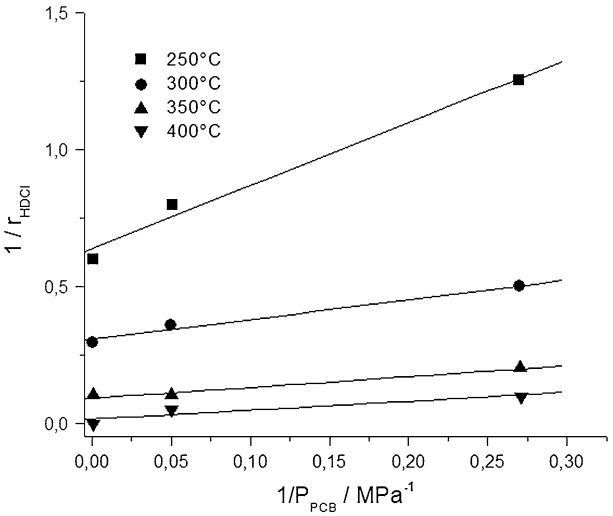

Fig. 6 $1/r_{HDCl}$ as a function of $1/P_{PCB}$. Mo/Al_2O_3 catalyst

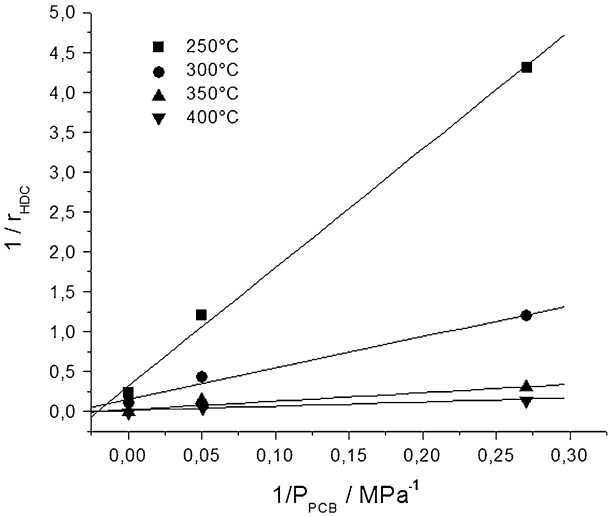

Fig. 7 $1/r_{HDCl}$ as a function of 1/PPCB. $Co–Mo/Al_2O_3$ catalyst

1.0 wt% exhibited linear relationships for the plots representing $1/r_{HDC}$ versus P_{H_2S} for both catalysts. Eq. 3 could be arranged to:

$$\frac{1}{r_{HDCl}} = \frac{K_{H_2S}P_{H_2S}}{k_{HDCl}K_{PCB}P_{PCB}} + \frac{(1 + K_{PCB}P_{PCB})}{k_{HDCl}K_{PCB}P_{PCB}} \quad (5)$$

From this expression, K_{H_2S} could be estimated from the slopes after calculating k_{HDC} and K_{PCB} from Eq. 4.

Figs. 8 and 9 show the effects of the H_2S partial pressure on the PCB HDC rates over the Mo/Al_2O_3 catalyst and the $Co–Mo/Al_2O_3$ catalyst, respectively. The HDC rates obtained over either catalyst decreased with increasing H_2S partial pressure, which means that the addition of H_2S inhibited the PCBs HDC reaction to a certain extent. As shown in Fig. 8, over the Mo/Al_2O_3 catalyst the PCB HDC rate under a H_2S partial pressure of 0.05×10^5 Pa decreased about 65 % when compared to the rate obtained without addition of H_2S at 300 °C.

In contrast, using the $Co–Mo/Al_2O_3$ catalyst, the PCB HDC rate under a H_2S partial pressure of 0.05×10^5 Pa decreased about 80 % when compared to the rate obtained without the addition of H_2S at 300 °C. These results show that the PCB HDC over the $Co–Mo/Al_2O_3$ catalyst was more strongly inhibited by H_2S than over the Mo/Al_2O_3 catalyst. Moreover, while the inhibition extent of H_2S over the Mo/Al_2O_3 catalyst was quite independent of the temperature (Fig. 8) that observed over the $Co–Mo/Al_2O_3$ catalyst became lower with increasing temperature (Fig. 9). This implies that the absolute value of the adsorption equilibrium constant between PCB and H_2S on the $Co–Mo/Al_2O_3$ catalyst was more influenced by an increase in temperature than the Mo/Al_2O_3 catalyst.

Arrhenius and Van't Hoff plots

To elucidate the reaction pathway of the inhibiting effect of H_2S on the HDC activity over Mo and Co–Mo catalysts, we estimated the activation energy of the HDC reaction from the activity results and subsequently calculated the heats of adsorption of PCB and H_2S using the Langmuir–Hinshelwood model. The rate constants of HDC (k_{HDC}) and the adsorption equilibrium constant of PCB (K_{PCB}) were calculated using Eq. 4, while the adsorption equilibrium constant of hydrogen sulfide K_{H_2S} was calculated using Eq. 5. Fig. 10 shows the Arrhenius plots for the PCB HDC reaction.

The activation energy calculated from the slopes for the Mo and the Co–Mo catalyst were 126 and 106 kJ mol^{-1}, respectively. Figs. 11 and 12 show the Van't Hoff plots for the PCB HDC over Mo and Co–Mo catalysts, respectively.

The heats of adsorption calculated from the slope of each line are summarized in Table 1. The heats of adsorption of PCB and H_2S on the Mo/Al_2O_3 catalyst were 14 and 38 kJ mol^{-1}, respectively, while the heats of adsorption of PCB and H_2S on the $Co–Mo/Al_2O_3$ catalyst were 31 and 128 kJ mol^{-1}, respectively.

While the value of the activation energy reflects the relative difficulty of the dechlorination of PCBs (Aroclor 1242), the values of the heat of adsorption reflect the relative strength of the adsorption of PCBs or H_2S on the catalysts. Considering this, from the values of the heat of adsorption of PCB and H_2S over Mo and Co–Mo catalysts, it seems that in both cases the adsorption of H_2S on the catalysts is stronger than that of PCB, which means that the PCB HDC is hindered to a certain extent. In particular, the heats of adsorption of BPC and H_2S were higher on the $Co–Mo/Al_2O_3$ catalyst than on the Mo/Al_2O_3 catalyst, suggesting that the addition of cobalt to Mo/Al_2O_3 catalysts makes easier the adsorption of sulfur on the surface of these catalysts.

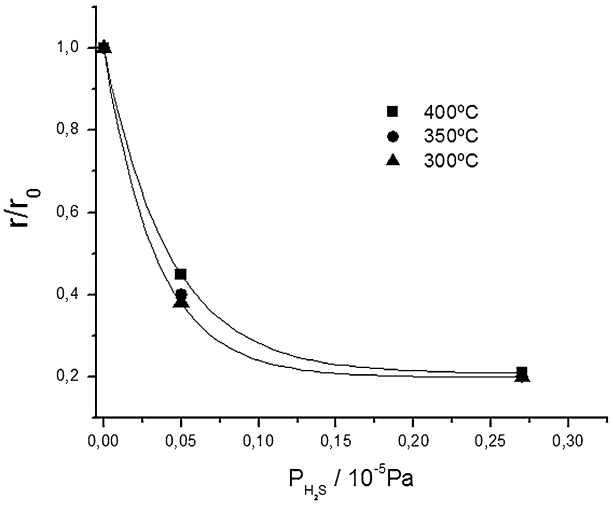

Fig. 8 Effect of the H_2S partial pressure on PCB HDC activity. Mo/Al_2O_3

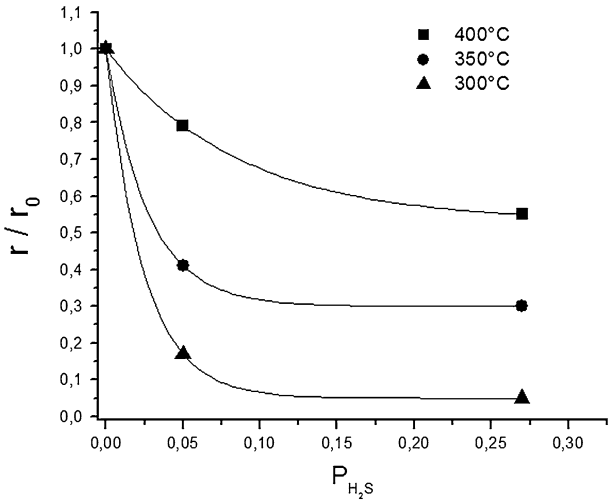

Fig. 9 Effect of the H_2S partial pressure on PCB HDC activity. $Co–Mo/Al_2O_3$

A reaction pathway of the PCB hydrodechlorination over alumina-supported molybdenum-based catalysts could be proposed. In the HDC working conditions at the steady state, PCB and the produced H_2S are both present in the system. Afterwards, PCB could be adsorbed on an active site, and then adsorbed species reacts with hydrogen to produce biphenyl. For a molybdenum catalyst, the heats of absorption of H_2S and PCB were smaller than the ones observed over the Co–Mo catalyst. While the heats of adsorption of H_2S are higher than those of PCBs, nevertheless, PCB dechlorination is observed, suggesting a relatively weak and

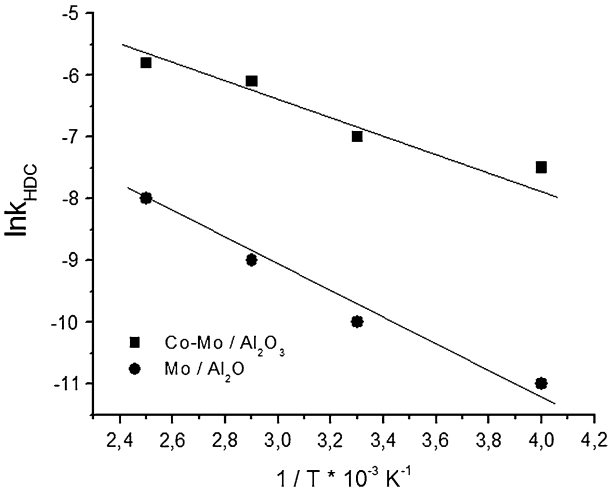

Fig. 10 Arrhenius plots

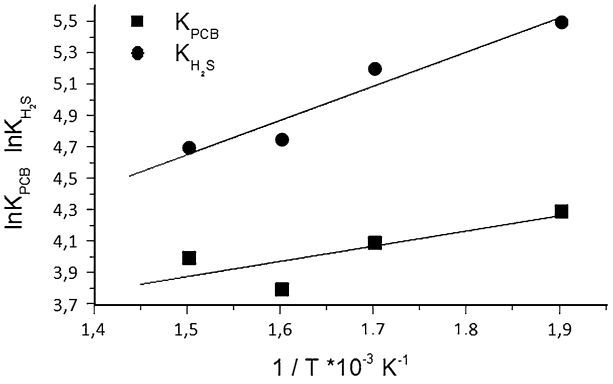

Fig. 11 Van't Hoff plots for the PCB and the H_2S adsorption equilibrium constants (Mo/Al_2O_3 catalyst)

dynamic adsorption of sulfur species. Thus, some PCBs molecules could be adsorbed on the (Co–)Mo catalyst surface and the reaction can further proceed in the same way as proposed above.

Assuming that while the H_2S poisoning is lower on the Mo catalyst, the number of active sites would be also smaller and the activity is therefore lower than the one observed over a Co–Mo catalyst. In this sense, the greater number of active sites of Co–Mo catalyst would be sufficient to compensate the H_2S hindrance.

We cannot exclude that the HDC rate deterioration induced by H_2S, might be better rendered by the kinetic modeling using improved fittings. As a consequence, to clarify the peculiar inhibition effect of H_2S on (Co–)Mo catalyst, we need further investigations. On the one hand, complementary experimental data are required to better understand the HDC reaction pathway on the commercial catalyst.

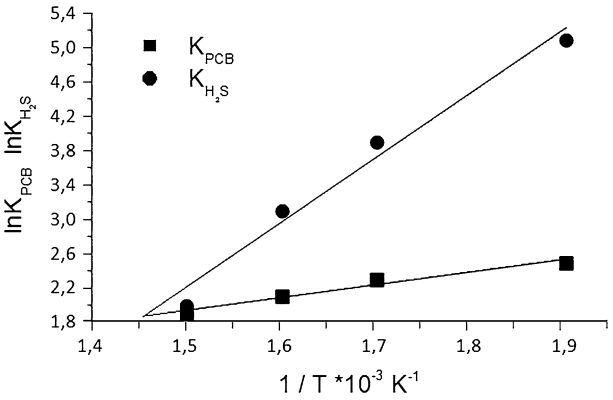

Fig. 12 Van't Hoff plots for the PCB and the H_2S adsorption equilibrium constants (Co–Mo/Al_2O_3 catalyst)

Table 1 Results of the kinetic treatments for catalysts

Catalyst	% Conversion	E_a kJ mol^{-1}	Q_{PCB} kJ mol^{-1}	Q_{H_2S} kJ mol^{-1}
Mo/Al_2O_3	14	126	14	38
Co–Mo/Al_2O_3	74	106	31	128

Conclusions

The effect of H_2S on the PCBs HDC activity of (Co–)Mo/Al_2O_3 catalysts was investigated. We have confirmed that the addition of cobalt remarkably promotes the HDC activity of a molybdenum catalyst. The HDC rates of both Mo and Co–Mo catalysts decreased with increasing partial pressure of H_2S. In particular, the Co–Mo/Al_2O_3 catalyst was more inhibited by H_2S than Mo/Al_2O_3 catalysts at 300 °C.

Some important kinetic parameters were calculated using the Langmuir–Hinshelwood equations. We found that the heat of adsorption of H_2S was larger than that of PCB on both catalysts, indicating that H_2S was adsorbed on the catalyst more strongly than PCB with the consequence of inhibiting the PCB HDC to a certain extent. Especially, the heats of adsorption of PCBs and H_2S on the Co–Mo catalyst were quite high (31 and 128 kJ mol^{-1}, respectively) compared with the Mo catalyst (14 and 38 kJ mol^{-1}, respectively), indicating that sulfur species adsorb with higher strength on the catalyst upon cobalt addition.

Acknowledgments This work was financed by research grants from FONACYT (G-2005000444), and PDVSA (Contract No. 2005-00051/2005-024).

References

1. Blais JM, Schindler DW, Muir DCG, Kimpe LE, Donald DB, Rosenberg B (1998) Accumulation of persistent organochlorine compounds in mountains of western Canada. Nature 395:585–588

2. Hites RA (1990) Environmental behavior of chlorinated dioxins and furans. Acc Chem Res 23:194–201
3. Erickson MD (1997) Analytical chemistry of PCB's, 2nd edn. CRC Press, Boca Raton, pp 1–96
4. Asante KA, Adu-Kumi S, Nakahiro K, Takahashi S, Isobe T, Sudaryanto A, Devanathan G, Clarke E, Ansa-Asare OD, Dapaah-Siakwan S, Tanabe S (2011) Human exposure to PCBs, PBDEs and HBCDs in Ghana: temporal variation, sources of exposure and estimation of daily intakes by infants. Environ Int 37(5):921–928
5. Domingo JL, Bocio A (2007) Levels of PCDD/PCDFs and PCBs in edible marine species and human intake: a literature review. Environ Int 33(3):397–405
6. Inventory of world-wide PCB destruction capacity, first issue, The Environment Programme of the United Nations, December 1998
7. Hitchman ML, Spackman R, Ross NC, Agra C (1995) Disposal methods for chlorinated aromatic waste. Chem Soc Rev 25:423–430
8. Erikson MD, Cole CJ, Flora JD Jr, Gorman PG, Haile CL, Hinsshaw GD, Hopkins FC, Swanson SE, Heggem DT (1985) PCDF formation from PCBs under fire. Chemosphere 14:855–858
9. Grosso M, Biganzoli L, Rigamonti L, Cernuschi S, Giugliano M, Poluzzi V, Biancolini V (2012) Experimental evaluation of PCDD/Fs and PCBs release and mass balance of a WTE plant. Chemosphere 86(3):293–299
10. Brunelle DJ, Mendiratta AK, Singleton DA (1985) Reaction/removal of polychlorinated biphenyls from transformer oil: treatment of contaminated oil with poly(ethylene glycol)/KOH. Environ Sci Technol 19:740–746
11. Roth JA, Dakoji SR, Hughes RC, Carmody RE (1994) Hydrogenolysis of polychlorinated biphenyls by sodium borohydride with homogeneous and heterogeneous nickel catalysts. Environ Sci Technol 28:80–87
12. Liu Y, Schwartz J, Cavallaro CL (1995) Catalytic dechlorination of polychlorinated biphenyls. Environ Sci Technol 29:836–840
13. Lassova L, Lee HK, Hor TSA (1999) Catalytic dechlorination of chlorobenzenes: effect of solvent on efficiency and selectivity. J Mol Catal A 144(3):397–403
14. Anwer MK, Spatola AF (1985) Applications of ammonium formate catalytic transfer hydrogenolysis—IV[1]: a facile method for dehalogenation of aromatic chlorocarbons. Tetrahedron Lett 26(11):1381–1384
15. Anwer MK, Sherman DB, Roney JG, Spatola AF (1989) Applications of ammonium formate catalytic transfer hydrogenation. 6. Analysis of catalyst, donor quantity, and solvent effects upon the efficacy of dechlorination. J Org Chem 54:1284–1289
16. Marques CA, Selva M, Tundo P (1994) Facile hydrodehalogenation with H2 and Pd/C catalyst under multiphase conditions. Part 2. selectivity and kinetics. J Org Chem 59:3830–3837
17. Sajiki H, Kume A, Hattori K, Nagaseb H, Hirota K (2002) Complete and truly catalytic degradation method of PCBs using Pd/C–Et_3N system under ambient pressure and temperature. Tetrahedron Lett 43(40):7251–7254
18. Yak HK, Wenclawiak BW, Cheng IF, Doyle JG, Wai CM (1999) Reductive dechlorination of polychlorinated biphenyls by zerovalent iron in subcritical water. Environ Sci Technol 33:1307–1310
19. Chuang F-W, Larson RA, Wessman MS (1995) Zero-valent ironpromoted dechlorination of polychlorinated biphenyls. Environ Sci Technol 29:2460–2463
20. Grittini C, Malcomson M, Fernand Q, Korte N (1995) Rapid dechlorination of polychlorinated biphenyls on the surface of a Pd/Fe bimetallic system. Environ Sci Technol 29:2898–2900
21. Wang C-B, Zhang W-X (1997) Synthesizing nanoscale iron particles for rapid and complete dechlorination of TCE and PCBs. Environ Sci Technol 31(7):2154–2156
22. Jackman SA, Knowles CJ, Robinson GK (1999) SACRED—a novel catalytic process for the environmental remediation of polychlorinated biphenyls (PCBS). Chemosphere 38(8):1889–1900
23. Zhang P-C, Scrudato RJ, Pagano JJ, Roberts RN (1993) Photodecomposition of PCBs in aqueous systems using TiO_2 as catalyst. Chemosphere 26(6):1213–1223
24. Arbon RE, Mincher BJ, Knighton WB (1994) γ-Ray destruction of individual PCB congeners in neutral 2-propanol. Environ Sci Technol 28:2191–2196
25. Arbon RE, Mincher BJ, Knighton WB (1996) γ-Ray destruction of individual PCBs in isooctane and transformer oil. Environ Sci Technol 30:1866–1871
26. Schmelling DC, Poster DL, Chaychian M, Neta P, Silverman J, Al-sheikhly M (1998) Degradation of poly-chlorinated biphenyls induced by ionizing radiation in aqueous micellar solutions. Environ Sci Technol 32:270–275

27. Chaychian M, Silverman J, Al-Shieikhly M (1999) Ionizing radiation induced degradation of tetrachlorobiphenyl in transformer oil. Environ Sci Technol 33:2461–2464
28. Simion AM, Miyata H, Kakeda M, Egashira N, Mitoma Y, Simion C (2013) Direct and complete cleansing of transformer oil contaminated by PCBs. Sep Purif Technol 103:267–272
29. Sediak DL, Andren AW (1991) Aqueous-phase oxidation of polychlorinated biphenyls by hydroxyl radicals. Environ Sci Technol 25:1419–1427
30. Zhang S, Rusling JF (1995) Dechlorination of polychlorinated biphenyls on soils and clay by electrolysis in a bicontinuous microemulsion. Environ Sci Technol 29:1195–1199
31. Huang Q, Rusling JF (1995) Formal reduction potentials and redox chemistry of polyhalogenated biphenyls in a bicontinuous microemulsion. Environ Sci Technol 29:98–103
32. Jain VK (1993) Supercritical fluids tackle hazardous wastes. Environ Sci Technol 27:806–808
33. Kim K, Kim KS, Hwan Son S, Cho J, Kim Y-C (2011) Supercritical water oxidation of transformer oil contaminated with PCBs—a road to commercial plant from bench-scale facility. J Supercrit Fluid 58(1):121–130
34. Hagh BF, Allen DT (1990) Catalytic hydrodechlorination. In: Freeman HM (ed) Innovative hazardous waste treatment technology. Technomic, Lancaster, p 45
35. Hagh BF, Allen DT (1990) Catalytic hydroprocessing of chlorinated benzenes. Chem Eng Sci 45:2695–2701
36. Hagh BF, Allen DT (1990) Catalytic hydroprocessing of chlorobenzene and 1,2-dichlorobenzene. AIChE J 36:773–778
37. Chon S, Allen DT (1991) Catalytic hydroprocessing of chlorophenols. AIChE J 37:1730–1732
38. Murena F (1997) Catalytic hydrodechlorination of monochlorobiphenyls using Ni–Mo/Gamma-Al_2O_3 sulphided catalyst. Environ Technol 18:317–324
39. Murena F, Schioppa E (2000) Kinetic analysis of catalytic hydrodechlorination process of polychlorinated biphenyls (PCBs). Appl Catal B Environ 27(4):257–267
40. Kim DI, Allen DT (1997) Catalytic hydroprocessing of chlorinated olefins. Ind Eng Res 36:3019–3026
41. Zhu K, Sun C, Chen H, Baig SA, Sheng T, Xu X (2013) Enhanced catalytic hydrodechlorination of 2,4-dichlorophenoxyacetic acid by nanoscale zero valent iron with electrochemical technique using a palladium/nickel foam electrode. Chem Eng J 223:192–199
42. Kalnes TN, James RB (1988) Hydrogenation and recycle of organic waste streams. Environ Prog 7:185–191
43. Brinkmann DW, Dickson JR, Wilkinson D (1995) Full-Scale hydrotreatment of polychlorinated biphenyls in the presence of used lubricating oils. Environ Sci Technol 29:87–91
44. Murena F, Gioia F (2002) Catalytic hydrodechlorination of decachlorobiphenyl. Appl Catal B Environ 38(1):39–50
45. LaPierre RB, Guczi L, Kranich WL, Weiss AH (1978) Hydrodechlorination of polychlorinated biphenyl. J Catal 52(2):230–238
46. Gissy H, Bartsch R, Tanielin C (1980) Hydrodesulfurization: IV. The effects of the feed components on Co–Mo/Al_2O_3 catalyst activation. J Catal 65(1):158–165
47. Yamada M, Shi YL, Obara T, Sakaguchi K (1990) Hydrogenation by CoMo/Al_2O_3 catalyst (Part 7) effects of catalyst pretreatment and H_2S on hydrodesulphurization of benzothiophene. Sekiyu Gakkaishi 33:227–233
48. Singhal GH, Espino RL, Sobel JE, Huff GA Jr (1981) Hydrodesulfurization of sulfur heterocyclic compounds: kinetics of dibenzothiophene. J Catal 67(2):457–468
49. Kabe T, Aoyama Y, Wang D, Ishihara A, Qian W, Hosoya M, Zhang Q (2001) Effects of H_2S on hydrodesulfurization of dibenzothiophene and 4,6-dimethyldibenzothiophene on alumina-supported NiMo and NiW catalysts. Appl Catal A Gen 209(1–2):237–247
50. Vrinat ML (1983) The kinetics of the hydrodesulfurization process—a review. Appl Catal 6(2):137–158
51. Afanasiev P (2010) The influence of reducing and sulfiding conditions on the properties of unsupported MoS_2-based catalysts. J Catal 269:269–280
52. Puello-Polo E, Brito JL (2010) Effect of the activation process on thiophene hydrodesulfurization activity of activated carbon-supported bimetallic carbides. Catal Today 149(3–4):316–320
53. ASTM D4059 (1991) Standard test method for analysis of polychlorinated biphenyls in insulating liquids by gas chromatography. ASTM, Baltimore

54. Choi YH, Lee WY (2000) Effect of Ni loading and calcination temperature on catalyst performance and catalyst deactivation of Ni/SiO_2 in the hydrodechlorination of 1,2-dichloropropane into propylene. Catal Lett 67:155–161
55. Park C, Menini C, Valverde JL, Keane MA (2002) Carbon–chlorine and carbon–bromine bond cleavage in the catalytic hydrodehalogenation of halogenated aromatics. J Catal 211(2):451–463
56. Keane MA (2002) Interfacial applications in environmental engineering. Marcel Dekker, New York, p 231
57. Gampine A, Eyeman DP (1998) Catalytic hydrodechlorination of chlorocarbons. 2. Ternary oxide supports for catalytic conversions of 1,2-dichlorobenzene. J Catal 179(1):315–325
58. Ohtsuka Y (1989) Influence of hydrogen chloride treatment on the dispersion of nickel particles supported on carbon. J Mol Catal 54(2):225–235
59. Hoang-Van C, Kachaya Y, Teichner SJ, Arnaud Y, Dalmon JA (1989) Characterization of nickel catalysts by chemisorption techniques, x-ray diffraction and magnetic measurements: effects of support, precursor and hydrogen pretreatment. Appl Catal 46(2):281–296